JOURNAL OF MATERIALS SCIENCE 26 (1991) 1391–1394

Elevated temperature mechanical properties of continuous metallic glass ribbon-reinforced glass-ceramic matrix composites

R. U. VAIDYA, K. N. SUBRAMANIAN
Department of Metallurgy, Mechanics and Materials Science, Michigan State University, East Lansing, MI 48824-1226, USA

Effect of temperature on the modulus of rupture of glass-ceramic matrix composites reinforced with very small volume fractions (~1%) of continuous metallic glass ribbons was studied. The failure modes in such composites were found to significantly depend on the test temperature. Variations in the strength of the matrix, and the interfacial shear strength between the matrix and the ribbons due to changes in the test temperature, were found to control the elevated temperature strength and failure mode of these composites.

1. Introduction

Reinforcement of brittle matrices with high-strength fibres results in dramatically improved mechanical properties such as increased toughness and high strain to failure. Recent developments [1–6] have led to a renewed interest in continuous fibre-reinforced ceramic matrix composites for high-temperature applications. Metallic glass reinforcements in the form of ribbons possessing large surface areas and large aspect ratios have been demonstrated to be very effective in enhancing the mechanical properties of glass-ceramic matrices [7, 8]. Even very small volume fractions of metallic glass reinforcements were found to improve 'he strength, elastic properties and fracture toughness of the glass-ceramic matrices quite significantly. One potential use of such composites is at elevated temperatures, because glass-ceramics do not exhibit softening, unlike the parent glass from which they are derived. Successful application of such metallic glass ribbon-reinforced glass-ceramic composites for high-temperature applications depends on the characterization of their mechanical response at elevated temperatures. An understanding of the failure mode at elevated temperatures is also important to make "lifetime" predictions.

2. Experimental procedure

Rectangular bar-shaped composite specimens (5 cm × 1.5 cm × 0.4 cm) were prepared by using Corning Glass Code 7572 as the matrix and METGLAS®* MT 2605S-2 continuous ribbons as the reinforcements. The specimens were prepared by cold pressing and sintering techniques. Details of the chemical compositions of the ribbon and matrix, and composite manufacturing techniques have been described elsewhere [7].

Three-point bending tests were carried out in an Instron testing machine with a crosshead speed of 0.05 cm min^{-1}, in accordance with ASTM standard C-203/85. Elevated temperature tests were carried out by heating the specimen and the test fixture, with an electrical resistance furnace. The temperature of the furnace was controlled to within 5 °C. The specimens were soaked at the test temperature for 30 min prior to the tests. All the bending tests were performed in a nitrogen atmosphere to prevent oxidation of the fixture. A total of three specimens were tested at each temperature. Pull-out tests were also carried out at various temperatures to measure the ribbon–matrix interfacial bond strength.

3. Results and discussion

Plots of the modulus of rupture (MOR) of the unreinforced matrix and composite specimens as a function of test temperature are provided in Fig. 1. All the specimens were observed to retain most of their room-temperature strength even at about 400 °C. The composite specimens exhibited higher MOR values as

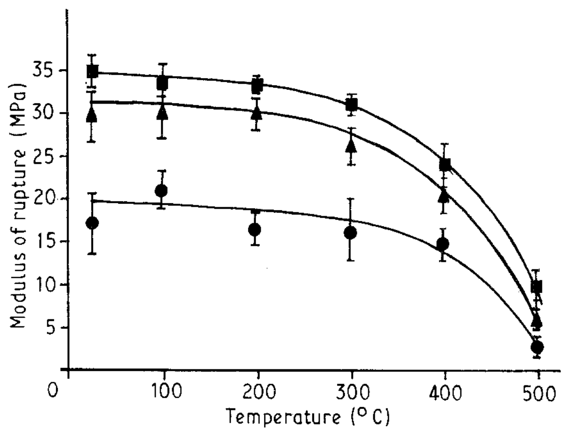

Figure 1 Plot of the modulus of rupture of the matrix and composite specimens as a function of temperature. (●) Matrix, (▲) composite with 0.73 vol % ribbons, (■) composite with 1.25 vol % ribbons.

* METGLAS® is a registered trademark of Allied Signal Inc for amorphous metallic alloys and brazing alloys

0022–2461/91 $03.00 + .12

compared to the unreinforced glass-ceramic matrix specimens at all temperatures tested. At higher temperatures matrix creep became predominant.

The load–deflection curves of the unreinforced matrix and composite specimens (containing 1.25 vol % reinforcements) at various temperatures are shown in Figs 2 and 3, respectively. At lower temperatures (up to 200 °C) the composite exhibited typical brittle behaviour, with no evidence of ribbon–matrix debonding and sliding. At 300 °C, a dramatic change was observed in the load–displacement curve, with the composite exhibiting ribbon debonding and sliding, accompanied by a large elongation to failure. At 400 °C, although the matrix began to creep, the composite still retained a large portion of its strength. At 500 °C, extensive matrix creep occurred and the composite failed at a very low load.

The observed changes in the load–displacement curves are an indication of the change (decrease) in the ribbon–matrix interfacial bond strength. These changes in the interfacial bond strength (with temperature) also have a significant effect on the load-transfer characteristics between the matrix and the ribbons which, in turn, affects the failure mode of the composite itself. In order to understand fully this phenomenon, the mechanism of load transfer from the matrix to the ribbon needs to be understood.

The ultimate load-bearing capacity of ceramic matrix composites is usually determined by the strength of the reinforcement (because the matrix cracks at a much smaller strain). It is, however, the onset of matrix cracking which is of significance, because it signifies the onset of permanent damage and loss of protection provided by the matrix against oxidation and corrosion of the reinforcements. Hence the matrix cracking stress is likely to be used as a design stress in future applications. For composite systems in which the reinforcements have the larger failure strain (and stress), the failure mode of the matrix (and hence the composite) is found to depend on the volume fraction of the reinforcements [9]. For volume fractions of reinforcements smaller than a "critical" volume fraction, single fracture of the matrix is observed. In this case failure of the matrix leads to composite failure, because the reinforcements are unable to carry the load when the matrix cracks. For volume fractions of reinforcements greater than the critical volume fraction, failure of the matrix does not lead to composite failure because the reinforcements can still carry the load. The failure mode of the matrix (and hence the composite) changes to one of multiple fracture. The "critical" volume fraction can be obtained by a simple load-balance equation and can be written as

$$V_c = \frac{\sigma_m^*}{\sigma_f^* - \sigma_f' + \sigma_m^*} \quad (1)$$

where σ_m^* is the fracture strength of the matrix, σ_f^* the fracture strength of the ribbon, and σ_f' the stress transferred to the ribbons when the matrix cracks.

For large reinforcement strains (exceeding the matrix failure strain), the matrix is observed to crack into blocks of fixed lengths [10, 11]. This length can be obtained by considering the load transfer between the reinforcements (ribbons) and the matrix. For the geometry of the ribbon reinforcements, because the load transfer across the ribbon matrix interface occurs by shear

$$N\tau 2(wx + tx) = \sigma_m^* A_m \quad (2)$$

where N is the total number of ribbons (continuous), τ the interfacial shear strength, σ_m^* the matrix cracking stress, A_m the cross-sectional area of the matrix, w the width of the ribbons, t the thickness of the ribbons, and x the length of the blocks into which the matrix cracks (which will be equal to the length of the ribbon initially). Solving for x

$$x = \frac{\sigma_m^* A_m}{2N\tau(w + t)} \quad (3)$$

Multiplying the numerator and denominator by wt (a constant)

$$x = \frac{\sigma_m^* A_m wt}{2N\tau(w + t)wt} \quad (4)$$

Now, Nwt is the total cross-sectional area of the ribbons (A_r).

Dividing numerator and denominator by the cross-sectional area of the composite (A_c)

$$x = \frac{\sigma_m^*(A_m/A_c)wt}{2\tau(w + t)(A_r/A_c)} \quad (5)$$

Because the composites are continuously reinforced, the volume fraction is equal to the area fraction. Hence

$$x = \frac{V_m \sigma_m^* wt}{V_r 2\tau(w + t)} \quad (6)$$

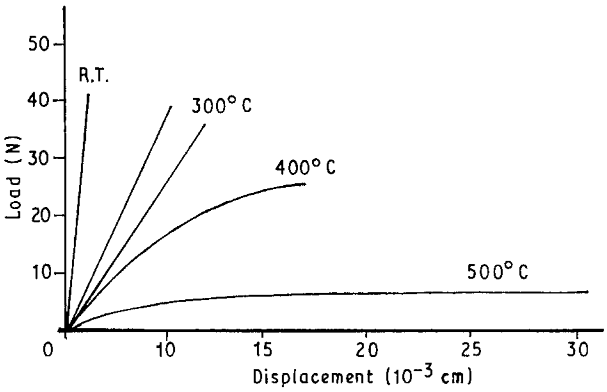

Figure 2 The load–displacement curves of the matrix specimens at various temperatures.

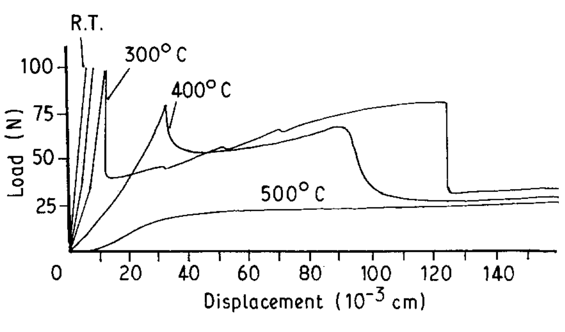

Figure 3 The load–displacement curves of the composite specimens (V_f = 1.25 vol %) at various temperatures.

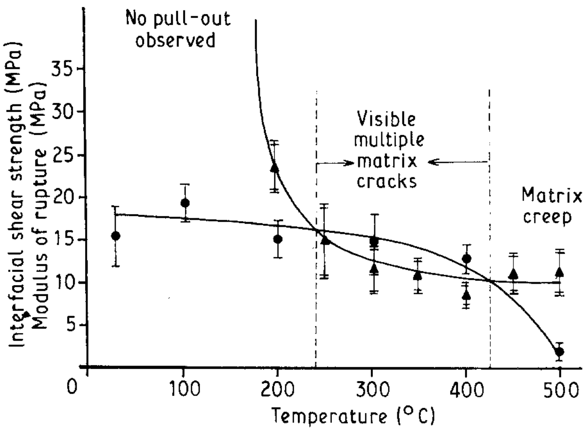

Figure 4 (●) Matrix strength and (▲) interfacial shear strength at various temperatures.

As x is a function of both σ_m^* and τ (for a given volume fraction and ribbon dimensions), the failure mode (single matrix crack or multiple matrix crack) will vary depending on the values of σ_m^* and τ.

The results of the pull-out tests carried out at various temperatures are provided in Fig. 4. Ribbon pull out was observed only at temperatures exceeding 250 °C. The matrix strength measured at various temperatures is also plotted in the same figure. Some of the interesting features that can be observed from this figure are as follows. Temperature influences both the matrix strength and interfacial shear strength. While the matrix strength was fairly constant up to 400 °C, the interfacial shear strength decreased sharply at about 250 °C. In an intermediate range from 300 to 400 °C, the interfacial shear strength was lower than the matrix strength. At temperatures above 400 °C, the matrix strength decreased rapidly while the interfacial shear strength exhibited only a moderate decrease. These changes lead to changes in the failure mode.

Visual observations of the composite specimens revealed that specimens tested at temperatures below 200 °C exhibit a single matrix crack in composite failure (Fig. 5a). At 300 °C, the failure mode of the matrix changes to one of multiple matrix cracking (Fig. 5b). Above 400 °C, although the interfacial strength was still decreased, the matrix strength was decreased more rapidly due to matrix creep. Hence the failure mode of the composite changed back to one of a single crack (Fig. 5c).

The effects of changes in the interfacial shear strength on ribbon pull out can be observed in the scanning electron micrographs shown in Figs 6 and 7. For the specimens tested at temperatures below 300 °C, no pull out was visible (Fig. 6a and b) and a

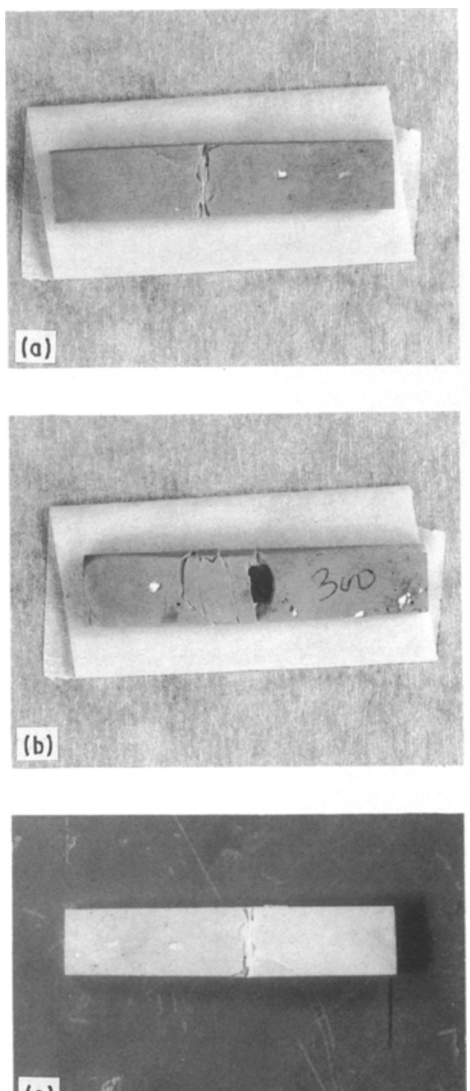

Figure 5 Composite failure modes at various temperatures. (a) Single crack observed at 200 °C. (b) Multiple matrix cracks observed at 300 °C. (c) Single crack observed at 400 °C.

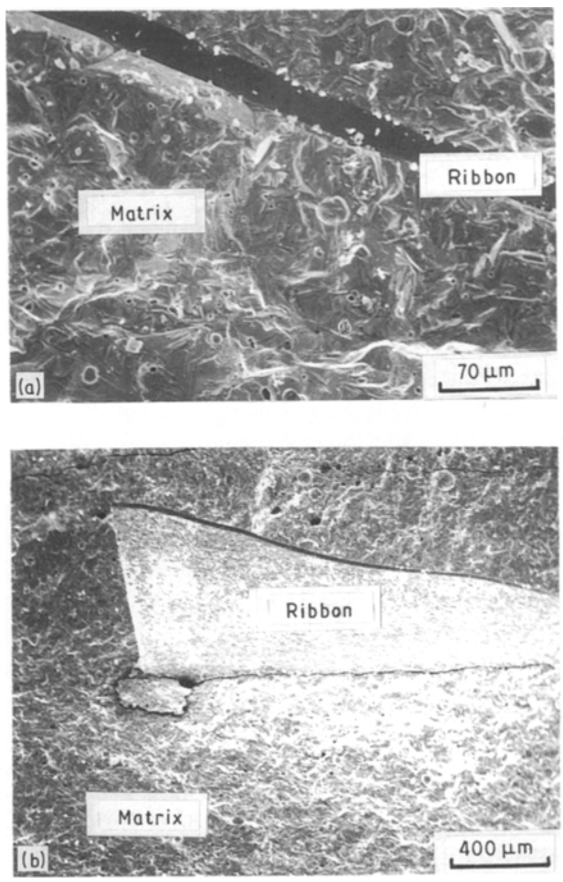

Figure 6 Micrographs illustrating the strong interfacial bonding for specimens tested below 300 °C. (a) presence of a strong void-free bond between the ribbon and the matrix; (b) absence of ribbon debonding and pull out.

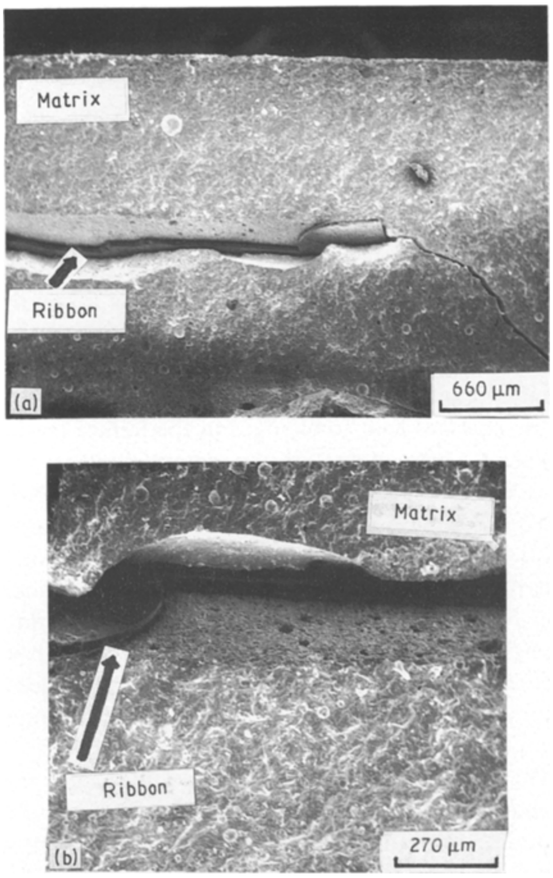

Figure 7 Micrographs showing ribbon–matrix debonding and ribbon pull out for specimens tested at 300 °C: (a) extensive ribbon debonding and pull out. A crack is observed to initiate at the edge of the ribbon; (b) a high magnification micrograph illustrating the smooth matrix surface in the debonded region.

strong ribbon–matrix interface was observed. At 300 °C, weakening of the interface was evinced accompanied by some ribbon sliding (Fig. 7a and b). The ribbon–matrix debonding and sliding was even more pronounced in the specimens tested at 400 °C (Fig. 8). This ribbon–matrix debonding and sliding provides for additional energy absorption and increased fracture toughness, at temperatures where there is no significant loss of matrix strength.

Hence the metallic glass reinforcements not only improve the strength and toughness of the glass-ceramic matrices at lower temperatures, but also provide for high-temperature toughness by means of interface-related effects such as debonding and pull out. Although the metallic glass ribbon/glass-ceramic matrix combination used in the present study had relatively lower temperature capabilities, proper choice of the matrix and reinforcement could be used to produce composites with high-temperature structural capabilities.

4. Conclusion

The failure mode of the metallic glass-reinforced glass-ceramic matrix composites changes with temperature

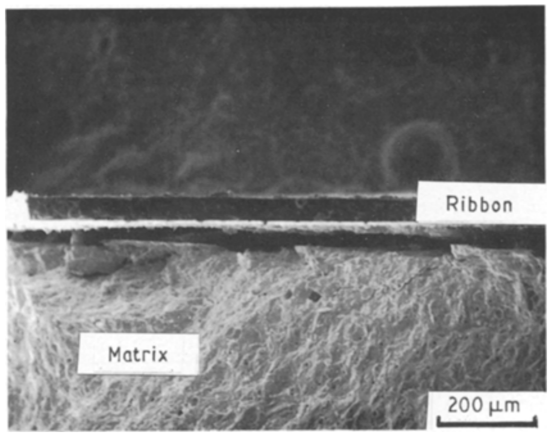

Figure 8 Micrograph of the extensive ribbon–matrix debonding and ribbon pull out in a specimen tested at 400 °C.

because of changes in the interfacial shear strength and matrix strength (with temperature). These changes in the failure mode of the composites provide for additional energy absorption, which, in turn, increases the fracture toughness of these composites.

Acknowledgements

The authors thank the Composite Materials and Structures Center, Michigan State University, for supporting and funding this project, Dr Kenneth Chyung, Corning Glass Works, and Dr Edward Norin, Metglas Products, for their valuable help and suggestions.

References

1. K. M. PREWO, *J. Mater. Sci.* **22** (1987) 2695.
2. E. Y. LUH and A. G. EVANS, *J. Amer. Ceram. Soc.* **70** (1987) 466.
3. R. W. RICE, *Ceram. Engng Sci. Proc.* **2** (1978) 694.
4. L. M. SHEPPARD, *Adv. Mater. Proc.* (incorporating *Metals Progr.*) **130** (1966) 54.
5. *Idem., ibid.* **130** (1966) 64.
6. K. M. PREWO, J. J. BRENNAN and G. K. LAYDEN, *Amer. Ceram. Soc. Bull.* **65** (1986) 305.
7. R. U. VAIDYA and K. N. SUBRAMANIAN, *J. Mater. Sci.* **25** (1990) 3291.
8. *Idem.*, in ASM/ACCE/ESD Conference Proceedings, Detroit, (American Society of Metals, Metals Park, Ohio, 1989) p. 227.
9. D. HULL, in "An introduction to composite materials", edited by R. W. Cahn, M. W. Thompson and I. M. Ward (Cambridge University Press, Cambridge, 1981) p. 125.
10. J. AVESTON, G. A. COOPER and A. KELLY, in "National Physics Laboratory Conference Proceedings" (IPC Science and Technology Press, Guildford, UK, 1971) p. 15.
11. D. B. MARSHALL, B. N. COX and A. G. EVANS, *Acta Metall.* **33** (1985) 2013.

Received 3 October 1989
and accepted 9 April 1990